JOURNAL OF GUIDANCE, CONTROL, AND DYNAMICS
Vol. 29, No. 3, May–June 2006

Asymptotic Analysis of Quasi-Equilibrium Glide in Lifting Entry Flight

Ping Lu*
Iowa State University, Ames, Iowa 50011-2271

The physical phenomenon of near equilibrium glide in entry flight of a lifting vehicle has long been a very useful utility in flight mechanics analysis and entry guidance designs. But no rigorous mathematical characterization of this quasi-equilibrium flight condition exists that can help provide a deeper understanding of when and how such a flight condition takes place and what is the precise relationship between exact and quasi-equilibrium glide. We present a formal analysis to quasi-equilibrium entry flight in this paper. We embed the quasi-equilibrium gliding flight problem in a class of regular perturbation problems and obtain solutions in asymptotic expansions. We show that the zeroth-order solution is an exact equilibrium glide solution. We provide the complete solution structure and convergence analysis. Our analysis yields quantitative accuracy estimates to the quasi-equilibrium glide condition that can guide how this approximation can be best used. The solution structure we obtain naturally leads to what can be done to improve the accuracy of the quasi-equilibrium glide condition.

I. Introduction

THE notion of equilibrium glide was first introduced in the analysis of hypervelocity lifting flight by the German rocket scientist Sänger as early as the 1930s.[1,2] The physical basis is that in gliding flight the vertical component of the acceleration tends to be small, and the flight-path angle is likely to be small. Therefore the flight-path angle and its rate can be approximated by zero in the differential equation governing the flight-path angle. The differential equation is thus reduced to an algebraic equation, known as the equilibrium glide condition (EGC). The EGC provides a very useful relationship between the altitude and velocity along the trajectory. It has been used in the entry trajectory analysis in the classic work by Chapman,[3] Eggers et al.,[4] and many others. The EGC continues to be a powerful tool that enables critical reduction of the dimension and complexity of flight mechanics problems, leading to various closed-form solutions that would otherwise not be attainable.[5,6] In the shuttle entry guidance design, the EGC is explicitly employed to define the lower boundary of the entry flight corridor within which the entry trajectory must lie in the velocity-drag acceleration space.[7] In all of these cases where the EGC is used, the vehicle is not exactly in equilibrium glide, which requires the vehicle to maintain a constant flight-path angle. Rather, the flight-path angle is actually time varying, in most cases with small-amplitude phugoid oscillations. In this sense, such a flight condition should be more appropriately referred to as quasi-equilibrium glide and the EGC as quasi-equilibrium glide condition (QEGC). Most recently, the concept of quasi-equilibrium glide is further expanded to allow the inclusion of time-varying bank angle.[8] Creative utilization of the QEGC in such a context constitutes the cornerstone for a fast and capable planning algorithm for fully constrained three degrees-of-freedom entry trajectories in Ref. 8.

Despite numerous successful applications of the QEGC in analyses as well as in engineering practice of lifting entry flight, there has not been a mathematically rigorous and unambiguous characterization of the QEGC in the open literature. Realizing the fact that a physical entry trajectory does not have a constant or zero flight-path angle, all accept the QEGC as an approximation. But the nature of the approximations arising from the QEGC goes beyond simply ignoring small flight-path angle. The actual profiles of the altitude, velocity, and bank angle in general are different from those in exact equilibrium glide. So when these actual profiles are used in the QEGC, they also introduce approximations. The fundamental questions unanswered include under what conditions and in what sense the QEGC can be considered a valid approximation; where the limitations of the QEGC as an approximation lie; and what is the precise relationship between an exact equilibrium glide trajectory and a quasi-equilibrium glide trajectory. Satisfactory answers to these questions will change the current sole reliance on the heuristic arguments for the use of QEGC and empirical justifications. A clear understanding of the preceding issues not only has theoretical significance, but can also yield guidelines for more appropriate applications of the QEGC as a simplification tool and motivate ways to improve the accuracy of the QEGC when needed.

In this paper we provide a formal analysis to quasi-equilibrium lifting entry flight in longitudinal direction. We will first develop a quantitative characterization of quasi-equilibrium glide by the closeness of the trajectory to an exact equilibrium glide trajectory. For any given quasi-equilibrium glide trajectory, we formulate a family of regular perturbation problems, which include the given problem as a special case. This formulation prompts us to seek the solutions in the form of asymptotic expansions, one of which is the solution to the quasi-equilibrium glide trajectory under consideration. We will provide the general structures of the terms in the expansion and complete the process with a discussion on the asymptotic convergence of the expansion. The solution structure we obtain shows that the trajectory in quasi-equilibrium glide can be represented by the sum of an exact equilibrium trajectory and higher-order solutions.The well-known QEGC is derived as a zeroth-order approximation to the exact equilibrium glide trajectory. The analysis leads to quantitative estimates by which the accuracy of the trajectory parameters computed from the QEGC can be judged. The knowledge of these accuracy estimates in turn provides clear guidelines to the scope of applicability and limitations of the QEGC. On the basis of the trajectory solution structure obtained, we show how the accuracy of the QEGC can be further increased if necessary. Numerical illustrations of the analytical results using the space shuttle vehicle model are given to verify the development.

II. Longitudinal Dynamics and Equilibrium Glide

A. Longitudinal Dynamics

For analysis purposes, let us consider the dimensionless longitudinal equations of motion of a lifting entry vehicle over a spherical Earth:

$$\dot{r} = V \sin\gamma \tag{1}$$

Received 26 January 2005; accepted for publication 9 June 2005.

*Professor, Department of Aerospace Engineering, 2271 Howe Hall; plu@iastate.edu. Associate Fellow AIAA.

$$\dot{V} = -D - \sin\gamma/r^2 \tag{2}$$

$$\dot{\gamma} = (1/V)[L\cos\sigma + (V^2 - 1/r)(\cos\gamma/r)] \tag{3}$$

where r is the radial distance from the center of the Earth to the vehicle, normalized by the radius of the Earth $R_E = 6{,}378{,}135$ m. Sometimes r is referred to as the "altitude" in this paper without further distinguishing the obvious difference. The Earth-relative velocity V is normalized by $V_c = \sqrt{(g_0 R_E)}$ with $g_0 = 9.81$ m/s^2. The relative flight-path angle is γ, and σ is the bank angle, both in radians. The terms D and L are the aerodynamic drag and lift accelerations in g, defined by

$$D = \frac{\rho_0 V_c^2 S_{\text{ref}} C_D}{2mg_0}\bar{\rho}(r)V^2 := D_s\bar{\rho}(r)V^2 \tag{4}$$

$$L = \frac{\rho_0 V_c^2 S_{\text{ref}} C_L}{2mg_0}\bar{\rho}(r)V^2 := L_s\bar{\rho}(r)V^2 \tag{5}$$

where ρ_0 is a constant, typically the atmospheric density $\rho(r)$ at the sea level, and $\bar{\rho}(r) = \rho(r)/\rho_0$ is the normalized atmospheric density at the altitude r. The vehicle reference area is S_{ref} and m the mass of the vehicle. The drag and lift coefficients C_D and C_L can be functions of the angle of attack α and Mach number. The differentiation in Eqs. (1–3) is with respect to the dimensionless time t, which is the real time (sec) normalized by $\sqrt{(R_E/g_0)}$. The normalization in Eqs. (1–3) renders the range of variations in r for entry flight near unity, the variations of V from near unity to about 0.1, and the total time of entry flight at about 2. That is, their maximum values are on the same order of magnitude.

The omission of the Coriolis acceleration term as a result of Earth rotation in Eq. (2) produces an error on the order of 10^{-4} g in magnitude at most, and thus will be well justified for our purposes in this paper. The ignored Earth rotation terms in Eq. (3) would be on the order of 10^{-2} g at the beginning of the entry trajectory and decrease along the trajectory. Hence the Earth rotation terms in Eq. (3) have magnitudes comparable to or smaller than the order of accuracy that will be shown in the later sections of this paper. Therefore the omission of the Earth rotation effects should not alter the accuracy estimates to be obtained in this paper.

Let $\mathcal{U} \subset R^2$ be the admissible set for the trajectory controls $\{\sigma \;\; \alpha\}$, and $\mathcal{S} \subset R^2$ be the admissible set for $\{r \;\; V\}$. The set $\mathcal{S}$ is typically defined by the vehicle operational limits and constraints on heat rate, temperature, load factor, and dynamic pressure.[7,8] Both $\mathcal{U}$ and $\mathcal{S}$ are assumed to be closed and bounded. The definition of equilibrium glide in entry flight is stated in the following section.

B. Equilibrium Glide

Suppose that the initial conditions for r and V are specified at a given $t_0 \geq 0$, denoted by $r^{(0)}$ and $V^{(0)}$, respectively. In a fixed interval of interest $[t_0, T]$, the vehicle is said to be in equilibrium glide at a constant $\gamma_c < 0$ if for $\gamma(t_0) = \gamma_c$ an admissible trajectory control pair $\{\sigma_c(t) \;\; \alpha_c(t)\} \in \mathcal{U}$, $\forall t \in [t_0, T]$ can be found, such that the solution $\{r_c(t) \;\; V_c(t)\} \in \mathcal{S}$ to the following differential-algebraic equation system exists:

$$\dot{r}_c = V_c \sin\gamma_c, \qquad r_c(t_0) = r^{(0)} \tag{6}$$

$$\dot{V}_c = -D_s\bar{\rho}(r_c)V_c^2 - \sin\gamma_c/r_c^2, \qquad V_c(t_0) = V^{(0)} \tag{7}$$

$$L_s\bar{\rho}(r_c)V_c^2\cos\sigma_c + \left(V_c^2 - 1/r_c\right)(\cos\gamma_c/r_c) = 0 \tag{8}$$

The relationship in Eq. (8) is the EGC. The physical interpretation of equilibrium glide is that starting from the given altitude and velocity an appropriate constant flight-path angle $\gamma_c < 0$ can be found, so that, if initiated at this flight-path angle, the vehicle can maintain the trajectory at the same flight-path angle throughout $[t_0, T]$ by modulating the bank angle and/or angle of attack. This assumption makes no demand on the uniqueness of γ_c and $\{\sigma_c(t) \;\; \alpha_c(t)\}$. In fact, if a γ_c and the corresponding pair $\{\sigma_c(t) \;\; \alpha_c(t)\}$ satisfy the preceding conditions and no portions of the resulting $\{r_c(t) \;\; V_c(t)\}$ and $\{\sigma_c(t) \;\; \alpha_c(t)\}$ are on the boundaries of their respective admissible sets, there will be a range of neighboring values for γ_c and $\{\sigma_c(t) \;\; \alpha_c(t)\}$ that will also meet the preceding conditions of equilibrium glide. This is a result of continuous dependence of the solutions of differential equations on parameters[9] and the smoothness of the DAEs involved. Note that no smallness of $|\gamma_c|$ is assumed, though this magnitude will most probably be small.

For short flight of a glider with high lift-to-drag (L/D) ratio, it is even possible to modulate simultaneously σ and α so that both γ and V remain constant in equilibrium glide. But entry vehicles have much smaller L/D values. Thus it is not physically possible to maintain constant V in any extended period in entry flight. The equilibrium glide condition (as well as the QEGC to be discussed) can only hold when there is sufficient dynamic pressure. This generally means that the equilibrium glide condition is only possible between the altitudes of approximately 40 to 80 km for entry flight.

To be definitive in the subsequent discussion, we will assume that the α profile is already given as a function of Mach number or V, as usually is the case in entry flight. This profile typically is determined on the basis of the considerations related to thermal protection and trim flight control. With this assumption, the only trajectory control is the bank angle σ.

A long-standing observation is that along many well-designed entry trajectories the flight-path angle and its rate are small in an extended portion of the flight. As a result, the QEGC is obtained by setting $\dot{\gamma} = \gamma = 0$ in Eq. (3) to get

$$L_s\bar{\rho}(r)V^2\cos\sigma + (V^2 - 1/r)(1/r) = 0 \tag{9}$$

In the early work,[1–4] Eq. (9) is used for two-dimensional flight in the vertical plane, and so $\sigma = 0$. The shuttle entry guidance design employs piecewise constant σ in this equation.[7] In Ref. 8 the QEGC is used in two ways: 1) finding the corresponding value of σ at a given pair of $\{r, V\}$; and 2) computing the corresponding altitude for a specified pair of $\{\sigma, V\}$. Because γ cannot be constantly zero along any entry trajectory, the QEGC in Eq. (9) can only be an approximation [an exception is the case when the bank angle profile σ is directly solved from Eq. (9) at the current r and V]. A main objective of this paper is to provide a formal analysis to quantify this approximation.

III. Formulation of the Problem

We consider in this paper a lifting entry trajectory that has the initial conditions $\{r^{(0)}, V^{(0)}, \gamma^{(0)}\}$ and a specified bank angle profile $\sigma(t)$ in a fixed finite interval $[t_0, T]$. The following assumption is a basic requirement in our development.

A. Assumption

Starting at the altitude $r(t_0) = r^{(0)}$ and velocity $V(t_0) = V^{(0)}$, a $\gamma_c < 0$ and the corresponding admissible bank angle profile $\sigma_c(t)$ can be found so that, when $\gamma(t_0) = \gamma_c$, an equilibrium glide trajectory $\{r_c(t) \;\; V_c(t) \;\; \gamma_c\}$ as defined in Eqs. (6–8) exists in $[t_0, T]$.

As pointed out in the preceding section, if there exists one pair $\{\gamma_c, \sigma_c(t)\}$ satisfying the preceding assumption, more such pairs can be found. Typically the range of the values for such γ_c is on the order of 10^{-3} (about 0.5–1 deg). For a given vehicle, the interval of interest $[t_0, T]$, and the specified initial conditions $r^{(0)}$ and $V^{(0)}$, the range of the possible values for γ_c can be easily determined numerically (see the example in Sec. IV). We can denote the set of all such γ_c by $\Gamma_c[r^{(0)}, V^{(0)}]$, where the dependence of this set on $r^{(0)}$ and $V^{(0)}$ is explicitly noted. The preceding assumption is equivalent to the condition that the set $\Gamma_c[r^{(0)}, V^{(0)}]$ is not empty. Next, let us denote the trajectory control by $u(t) = \cos\sigma(t)$ and $u_c(t) = \cos\sigma_c(t)$. The following definition is crucial in our problem formulation.

B. Definition of the Parameter ε_0

For the given initial conditions $\{r^{(0)}, V^{(0)}, \gamma^{(0)}\}$ and the trajectory control $u(t) = \cos\sigma(t)$, choose an appropriate pair $\{\gamma_c, u_c(t)\}$ as described in the preceding assumption. Define the parameter ε_0 by

$$\varepsilon_0 = \gamma^{(0)} - \gamma_c \tag{10}$$

The choice of the pair $\{\gamma_c, u_c(t)\}$ should be such that for the constant ε_0 a bounded function $\delta u(t)$ can be defined in $[t_0, T]$ so that the given trajectory control $u(t)$ can be expressed as

$$u(t) = u_c(t) + \varepsilon_0 \delta u(t) \tag{11}$$

Some elaborations on the preceding definition are in order. For the cases where the specified initial condition $\gamma^{(0)} \notin \Gamma_c[r^{(0)}, V^{(0)}]$, any pair of $\{\gamma_c, u_c(t)\}$ can be used, and $\delta u(t) = [u(t) - u_c(t)]/\varepsilon_0$ will be bounded. In the cases where $\gamma^{(0)}$ is the same as one of the possible values of γ_c, but $u(t)$ is different from the corresponding $u_c(t)$, a different pair $\{\gamma_c, u_c(t)\}$ should be chosen so that $\varepsilon_0 \neq 0$. The existence of a different pair $\{\gamma_c, u_c(t)\}$ has been ensured. Once a different pair is chosen, $\delta u(t) = [u(t) - u_c(t)]/\varepsilon_0$ will again be bounded. If $u(t)$ happens to be the same as some $u_c(t)$ defined in the assumption, but $\gamma^{(0)}$ is different from the corresponding γ_c, we will have $\varepsilon_0 = \gamma^{(0)} - \gamma_c \neq 0$ and $\delta u(t) \equiv 0$. Finally, if $\gamma^{(0)}$ is the same as one of the possible γ_c, and $u(t)$ is equal to the corresponding $u_c(t)$ for all $t \in [t_0, T]$, $\varepsilon_0 = \delta u(t) \equiv 0$ will satisfy the preceding definition. In short summary, the parameter ε_0 will be zero only when the given initial conditions and specified bank angle profile lead to an exact equilibrium glide trajectory. With the aid of the preceding definition, we can proceed to characterize the family of quasi-equilibrium glide trajectories under investigation in this paper in a more quantifiable fashion.

C. Quasi-Equilibrium Glide

The trajectory of a lifting entry vehicle is said to be in quasi-equilibrium glide in a given interval $[t_0, T]$, if the following two conditions hold true:

1) A parameter ε_0 as defined in the preceding definition can be found such that $|\varepsilon_0|$ is on the order of 10^{-2} or less.

2) The following condition is satisfied for a sufficiently small constant $k > 0$:

$$\left| \frac{\cos\sigma(t)}{\cos\sigma_c(t)} - 1 \right| < k < 1, \qquad \forall t \in [t_0, T] \tag{12}$$

where $\sigma_c(t)$ corresponds to the γ_c that defines ε_0 in condition 1.

The preceding order of magnitude for ε_0 translates into a range of 1 deg or so for $\gamma^{(0)} - \gamma_c$. The first condition indicates that the initial flight-path angle of a quasi-equilibrium glide trajectory should be reasonably close to a value from which an exact equilibrium glide is possible. Condition 2 stipulates that the difference between $\cos\sigma(t)$ and $\cos\sigma_c(t)$ should be sufficiently smaller than $|\cos\sigma_c(t)|$. The purpose of Eq. (12) is to ensure that the trajectory control σ will keep the trajectory in near-equilibrium glide in $[t_0, T]$, and the technical rationale will become apparent in Sec. IV.A. Although values of k in the range of 0.1–0.2 will most likely be sufficiently small, they might be too conservative in some cases. For a given length of the period $T - t_0$, the least conservative value of k can be estimated numerically by increasing the difference of $\cos\sigma - \cos\sigma_c$ until the asymptotic expansion to be introduced in Sec. IV.A stops to represent the trajectory. For example, for the space shuttle and $T - t_0 = 600$ s this process shows that the largest acceptable k is about 0.35. This value of k means that up to 20-plus degrees in the difference between σ and σ_c can be allowed, and the trajectory can still be regarded as in quasi-equilibrium glide.

The preceding qualifications define the type of quasi-equilibrium glide trajectories that we will examine in this paper. The actual choice of $\{\gamma_c, u_c(t)\}$ is not critical to our analysis because γ_c can only be in a small range (a degree or less), and our focus of study will be on the orders of magnitude. As will be seen in the next section, the preceding conditions set up an appropriate context for us to cast the quasi-equilibrium entry flight problems into regular perturbation problems in which the parameter ε_0 characterizes how far the actual trajectory is from an equilibrium glide trajectory. Consequently, the trajectory solutions in the form of asymptotic expansions can be sought as a logical step.

Asymptotic expansions have been a very useful tool in studying entry flight problems. One of the early works in this regard is by Shi and Pottsepp[10] in which two-dimensional entry flight solution is obtained using matched asymptotic expansions. The small parameter there is related to the scale height in the atmospheric density model. Separate expansions are done for vacuum and dense endoatmospheric portion of the trajectory with different scales in the independent variable (thus by a singular perturbation approach). The matched composite solution gives a continuous overall solution to the trajectory. With clever choice of certain motion variables, this approach is also used to obtain lifting entry solutions in three-dimensional motion.[11] Following the same formulation and technique, Ref. 12 later reports more trackable forms of three-dimensional solutions. For related research in aerospace guidance and control using singular perturbation methods, Ref. 13 provides a comprehensive recent survey.

The chief differences between the previous work[10–12] and the current paper lie in motivations, objectives, technical approaches, and final results. References 10–12 aim at obtaining analytical solutions to the motion variables along trajectories with constant L/D and bank angle. The approach used there is singular perturbation parameterized by an atmospheric density parameter. The results from Refs. 10–12 are approximate closed-form solutions that can be used for quick prediction of entry trajectories in guidance. In the present work, the objectives are to analyze the structure of entry trajectories in near-equilibrium glide, and quantify the accuracy of the QEGC in particular. Whether or not the trajectory solutions are in closed form is not a concern; thus, L/D and bank angle are allowed to be time-varying (as they generally are in actual entry flight). The perturbation problem is based on a parameter defining the closeness of the actual trajectory to an exact equilibrium glide trajectory. No timescale separation is necessary in this formulation. As a result, a regular perturbation approach is used. The products of the current analysis are a rigorous characterization of quasi-equilibrium gliding trajectories, the understanding of the accuracy and limitations of the QEGC in shaping and planning of entry trajectories, and a method to increase the accuracy of the QEGC if necessary.

IV. Asymptotic Expansion

For any quasi-equilibrium glide trajectory with given initial conditions $\{r^{(0)}, V^{(0)}, \gamma^{(0)}\}$ and a specified bank angle profile $\sigma(t)$, we first determine $\varepsilon_0 = \gamma^{(0)} - \gamma_c$ and $\delta u(t) = [\cos\sigma(t) - \cos\sigma_c(t)]/\varepsilon_0$ as described in the preceding section. We will then fix the profiles $\delta u(t)$ and $u_c(t) = \cos\sigma_c$ as determined and introduce a small parameter ε that is on the order of ε_0 but can vary independently. Let us define a family of ε-dependent trajectories for which the initial conditions and trajectory control are

$$\gamma(t_0) = \gamma_c + \varepsilon, \qquad r(t_0) = r^{(0)}, \qquad V(t_0) = V^{(0)} \tag{13}$$

$$u(t) = u_c(t) + \varepsilon \delta u(t), \qquad t \in [t_0, T] \tag{14}$$

Clearly the aforementioned particular quasi-equilibrium glide trajectory is embedded in this family of ε-dependent trajectories as one of the members, corresponding to the case when $\varepsilon = \varepsilon_0$. For any ε on the order of ε_0 or smaller and with the definition of δu from Eq. (11), it can be easily verified that the condition in Eq. (12) means the dominance of $u_c(t)$ over $\varepsilon\delta u(t)$ in the right-hand side of Eq. (14). Therefore the preceding problem can be considered a regular perturbation problem with ε as the perturbation variable. Let the state vector of the longitudinal dynamics in Eqs. (1–3) be $\boldsymbol{x} = (r \;\; V \;\; \gamma)^T$. We seek to represent the solution to this family of near-equilibrium glide trajectories by the asymptotic expansion of

$$\boldsymbol{x}(t, \varepsilon) = \begin{pmatrix} r \\ V \\ \gamma \end{pmatrix} = \begin{pmatrix} r_0 \\ V_0 \\ \gamma_0 \end{pmatrix} + \varepsilon \begin{pmatrix} r_1 \\ V_1 \\ \gamma_1 \end{pmatrix} + \varepsilon^2 \begin{pmatrix} r_2 \\ V_2 \\ \gamma_2 \end{pmatrix} + \cdots$$

$$:= \boldsymbol{x}_0 + \varepsilon \boldsymbol{x}_1 + \varepsilon^2 \boldsymbol{x}_2 + \cdots = \sum_{i=0}^{\infty} \varepsilon^i \boldsymbol{x}_i(t) \tag{15}$$

Once $\boldsymbol{x}(t, \varepsilon)$ is found, the solution to the original problem will simply be $\boldsymbol{x}(t, \varepsilon_0)$. The rest of this section is dedicated to finding $\boldsymbol{x}_i$,

$i = 0, 1, 2, \ldots$, and analyzing the asymptotic convergence of the power series in Eq. (15).

A. Construction of Solution

We will proceed to determine the terms in the expansion (15). Denote the right-hand sides of Eqs. (1–3) by $\boldsymbol{f}(\boldsymbol{x}, u)$. With the power series (15) for $\boldsymbol{x}$ and $u = u_c + \varepsilon\delta u$ in Eq. (14), we expand the function $\boldsymbol{f}[\boldsymbol{x}(t, \varepsilon), u_c + \varepsilon\delta u]$ by Taylor series at $\varepsilon = 0$:

$$\boldsymbol{f}[\boldsymbol{x}(t, \varepsilon), u_c+\varepsilon\delta u] = \boldsymbol{f}(\boldsymbol{x}_0, u_c)+\varepsilon\frac{\mathrm{d}\boldsymbol{f}}{\mathrm{d}\varepsilon}(\boldsymbol{x}_0, u_c)+\frac{\varepsilon^2}{2!}\frac{\mathrm{d}^2\boldsymbol{f}}{\mathrm{d}\varepsilon^2}(\boldsymbol{x}_0, u_c)+\cdots \tag{16}$$

where the first-order derivative is simple

$$\begin{aligned}\frac{\mathrm{d}\boldsymbol{f}}{\mathrm{d}\varepsilon}(\boldsymbol{x}_0, u_c) &= \left[\frac{\partial \boldsymbol{f}^T(\boldsymbol{x}, u)}{\partial \boldsymbol{x}}\frac{\partial \boldsymbol{x}(t, \varepsilon)}{\partial \varepsilon} + \frac{\partial \boldsymbol{f}(\boldsymbol{x}, u)}{\partial u}\frac{\partial u}{\partial \varepsilon}\right]_{\varepsilon=0} \\ &= \frac{\partial \boldsymbol{f}^T(\boldsymbol{x}_0, u_c)}{\partial \boldsymbol{x}}\boldsymbol{x}_1 + \frac{\partial \boldsymbol{f}(\boldsymbol{x}_0, u_c)}{\partial u}\delta u \\ &:= F(\boldsymbol{x}_0, u_c)\boldsymbol{x}_1 + \boldsymbol{\xi}_1(\boldsymbol{x}_0, \delta u)\end{aligned} \tag{17}$$

where

$$\boldsymbol{\xi}_1(\boldsymbol{x}, \delta u) = [0 \quad 0 \quad L_s\bar{\rho}(r)V\delta u]^T \tag{18}$$

The expression of $F(\boldsymbol{x}_0, u_c)$ is given in the Appendix. The higher-order derivatives will involve cross-product terms. The differentiations are tedious, yet straightforward nonetheless. This process shows that in general we have

$$\begin{aligned}\frac{\mathrm{d}^n\boldsymbol{f}}{\mathrm{d}\varepsilon^n}(\boldsymbol{x}_0, u_c) &= \left.\frac{\mathrm{d}^n\boldsymbol{f}}{\mathrm{d}\varepsilon^n}(\boldsymbol{x}, u)\right|_{\varepsilon=0} = n![F(\boldsymbol{x}_0, u_c)\boldsymbol{x}_n \\ &\quad + \boldsymbol{\xi}_n(\boldsymbol{x}_{n-1}, \boldsymbol{x}_{n-2}, \ldots, \boldsymbol{x}_0, u_c, \delta u)] \qquad n = 2, 3, \ldots\end{aligned} \tag{19}$$

where $\boldsymbol{\xi}_n$ is a well-defined smooth function of u_c, δu, and preceding solutions $\boldsymbol{x}_{n-1}(t), \ldots, \boldsymbol{x}_0(t)$. The expression for $\boldsymbol{\xi}_2$ is given in Appendix as an illustration.

The time derivatives of $\boldsymbol{x}$ are obtained in terms of $\dot{\boldsymbol{x}}_i$ by differentiating the series (15). Equating the coefficients of the like powers of ε in the equation

$$\dot{\boldsymbol{x}} = \sum_{i=0}^{\infty}\varepsilon^i\dot{\boldsymbol{x}}_i = \boldsymbol{f}(\boldsymbol{x}, u)$$

with $\boldsymbol{f}(\boldsymbol{x}, u)$ replaced by Eq. (16), we have the equations for determining $\boldsymbol{x}_i$, $i = 0, 1, 2, \ldots$.

It is straightforward to verify that the zeroth-order solution is

$$\boldsymbol{x}_0(t) = [r_c(t) \quad V_c(t) \quad \gamma_c]^T \tag{20}$$

where $r_c(t)$ and $V_c(t)$ are the altitude and velocity profiles from Eqs. (6) and (7) corresponding to the pair $\{\gamma_c, u_c(t)\}$. The assumption in Sec. III ensures the existence and boundedness of $\boldsymbol{x}_0(t)$.

Now $\boldsymbol{x}_0(t)$ is determined as a function of t and $u_c(t)$ already a continuous function of time defined in Eq. (8). With slight abuse of notation, we will use $F(t) = F[\boldsymbol{x}_0(t), u_c(t)]$ and $\boldsymbol{\xi}_1(t) = \boldsymbol{\xi}_1[\boldsymbol{x}_0(t), \delta u(t)]$ hereafter. Comparing the coefficients of ε in the preceding expansion results in the differential equation for the first-order solution $\boldsymbol{x}_1$ as follows:

$$\dot{\boldsymbol{x}}_1 = F(t)\boldsymbol{x}_1 + \boldsymbol{\xi}_1(t) \tag{21}$$

We choose the initial condition for $\boldsymbol{x}_1(t_0)$ to be

$$\boldsymbol{x}_1(t_0) = (0 \quad 0 \quad 1)^T \tag{22}$$

With this initial condition for $\boldsymbol{x}_1(t_0)$ and the initial condition $\boldsymbol{x}_0(t_0) = [r^{(0)} \quad V^{(0)} \quad \gamma_c]^T$ in Eqs. (6–8), the first two terms in the expansion (15) have recovered the full initial conditions given in Eq. (13), that is,

$$\boldsymbol{x}_0(t_0) + \varepsilon\boldsymbol{x}_1(t_0) = [r(t_0) \quad V(t_0) \quad \gamma(t_0)]^T = \boldsymbol{x}(t_0, \varepsilon) \tag{23}$$

Define the state transition matrix $\Phi(t, t_0) \in R^{3\times 3}$ by the solution of the matrix differential equation

$$\dot{\Phi}(t, t_0) = F(t)\Phi(t, t_0), \qquad \Phi(t_0, t_0) = I_{3\times 3} \tag{24}$$

Because $F(t)$ is continuous, so is $\Phi(t, t_0)$. The complete solution of $\boldsymbol{x}_1(t)$ to the differential system (21) with initial condition (22) is

$$\boldsymbol{x}_1(t) = \Phi(t, t_0)\boldsymbol{x}_1(t_0) + \int_{t_0}^{t}\Phi(t, \tau)\boldsymbol{\xi}_1(\tau)(\tau)\,\mathrm{d}\tau \tag{25}$$

At this point $\boldsymbol{x}_1(t)$ is completely determined in $[t_0, T]$. Because $\boldsymbol{\xi}_1(\,)$ is a continuous and bounded function, it follows that $\boldsymbol{x}_1$ is bounded on $[t_0, T]$.

The result in Eq. (19) indicates that the higher-order solutions are governed by the following linear differential equations:

$$\dot{\boldsymbol{x}}_j = F(t)\boldsymbol{x}_j + \boldsymbol{\xi}_j(\boldsymbol{x}_{j-1}, \boldsymbol{x}_{j-2}, \ldots, \boldsymbol{x}_0, u_c, \delta u) \tag{26}$$

$$\boldsymbol{x}_j(t_0) = 0, \qquad j = 2, 3, \ldots \tag{27}$$

The initial conditions in Eq. (27) are necessary because we must have

$$\boldsymbol{x}(t_0, \varepsilon) = \sum_{i=0}^{\infty}\varepsilon^i\boldsymbol{x}_i(t_0) = [r(t_0) \quad V(t_0) \quad \gamma(t_0)]^T \tag{28}$$

And the preceding condition is indeed satisfied [compare Eqs. (23) and (27)]. Note that the vector $\boldsymbol{\xi}_j(\cdots)$ in Eq. (26) is an already determined function of time from preceding solutions of $\boldsymbol{x}_i(t)$, $i = 0, 1, \ldots, j-1$, and so is $u_c(t)$, as well as $\delta u(t)$. In this sense we can again denote it by $\boldsymbol{\xi}_j(t)$. Then the solution for each $\boldsymbol{x}_j(t)$, $j = 2, 3, \ldots$, with the zero initial condition (27), can be expressed as

$$\boldsymbol{x}_j(t) = \int_{t_0}^{t}\Phi(t, \tau)\boldsymbol{\xi}_j(\tau)\,\mathrm{d}\tau \qquad j = 2, 3, \ldots \tag{29}$$

Because $\boldsymbol{x}_0$ and $\boldsymbol{x}_1$ are bounded, $\boldsymbol{\xi}_2(\boldsymbol{x}_1, \boldsymbol{x}_0, u_c, \delta u)$ is bounded on $[t_0, T]$. Thus $\boldsymbol{x}_2(t)$ must be bounded on $[t_0, T]$ from the preceding equation. Continuing this argument for $j \geq 3$ based on Eq. (29), it follows that all $\boldsymbol{x}_j$ are bounded on $[t_0, T]$. However, the boundedness of $\boldsymbol{x}_j$ is not the only concern for our purpose. We also need the asymptotic expansion (15) to remain valid in $[t_0, T]$ for $\varepsilon = \varepsilon_0$. To this end, we will need to ensure that the magnitudes of $\|\boldsymbol{x}_j(t)\|$, $j = 1, 2, \ldots$, are under reasonable bounds. These functions are strongly influenced by the magnitude of $|\cos\sigma(t) - \cos\sigma_c(t)|$ through the (linear) presence of δu in $\boldsymbol{\xi}_j$. This is why condition (12) is required in the problem formulation.

B. Asymptotic Convergence

The remaining task is to show that with the just obtained $\boldsymbol{x}_i$, $i = 0, 1, 2, \ldots$, the expansion on the right-hand side of Eq. (15) truncated after a fixed number of terms approaches the full solution $\boldsymbol{x}(t, \varepsilon)$ as $\varepsilon \to 0$. Such a property is referred to as asymptotic convergence of the power series (15).

Suppose that the expansion (15) is truncated after the Nth term, where $N \geq 2$. Denote the remainder of the expansion (15) at any $t \in [t_0, T]$ by $\varepsilon^N\boldsymbol{\eta}_N(t, \varepsilon) \in R^3$, where T is finite. We then have

$$\boldsymbol{x}(t, \varepsilon) - \sum_{k=0}^{N-1}\varepsilon^k\boldsymbol{x}_k(t) = \varepsilon^N\boldsymbol{\eta}_N(t, \varepsilon) \tag{30}$$

If we can show that $\boldsymbol{\eta}_N(t, \varepsilon)$ exists and is bounded on the interval $[t_0, T]$ for sufficiently small $|\varepsilon|$, the power series (15) is asymptotic. Because of the initial conditions (23) and (27) for $\boldsymbol{x}_k(t_0)$, the value of $\boldsymbol{\eta}_N$ at t_0 is given by

$$\boldsymbol{\eta}_N(t_0, \varepsilon) = \left[\boldsymbol{x}(t_0, \varepsilon) - \sum_{k=0}^{N-1}\varepsilon^k\boldsymbol{x}_k(t_0)\right]\Big/\varepsilon^N = 0 \tag{31}$$

Next, differentiate both sides of the relationship (30) to get

$$\varepsilon^N\dot{\boldsymbol{\eta}}_N = \dot{\boldsymbol{x}} - \sum_{k=0}^{N-1}\varepsilon^k\dot{\boldsymbol{x}}_k = \boldsymbol{f}(\boldsymbol{x},u) - \boldsymbol{f}(\boldsymbol{x}_0,u_c) - \sum_{i=1}^{N-1}\varepsilon^i(F\boldsymbol{x}_i+\boldsymbol{\xi}_i)$$

$$= \boldsymbol{f}(\boldsymbol{x}_0+\varepsilon\boldsymbol{x}_1+\cdots+\varepsilon^{N-1}\boldsymbol{x}_{N-1}+\varepsilon^N\boldsymbol{\eta}_N, u_c+\varepsilon\delta u)$$

$$-\boldsymbol{f}(\boldsymbol{x}_0,u_c) - \sum_{i=1}^{N-1}\varepsilon^i(F\boldsymbol{x}_i+\boldsymbol{\xi}_i) \tag{32}$$

We proceed to expand $\boldsymbol{f}(\boldsymbol{x}_0+\cdots+\varepsilon^{N-1}\boldsymbol{x}_{N-1}+\varepsilon^N\boldsymbol{\eta}_N, u_c+\delta u)$ by an Nth order Taylor series at $\varepsilon=0$:

$$\boldsymbol{f}(\boldsymbol{x}_0+\cdots+\varepsilon^N\boldsymbol{\eta}_N, u+\varepsilon\delta u) = \boldsymbol{f}(\boldsymbol{x}_0,u_c) + \sum_{i=1}^{N-1}\varepsilon^i(F\boldsymbol{x}_i+\boldsymbol{\xi}_i)$$

$$+\varepsilon^N[F\boldsymbol{\eta}_N+\boldsymbol{\xi}_N] + \varepsilon^{N+1}\boldsymbol{\ell}_N(\boldsymbol{\eta}_N,t,\theta\varepsilon) \tag{33}$$

where $\boldsymbol{\ell}_N$, a function of $\boldsymbol{\eta}_N, \boldsymbol{x}_{N-1}(t), \ldots, \boldsymbol{x}_0(t)$ and ε (note that the dependence on ε is also through $\boldsymbol{\eta}_N$), is the Lagrange remainder in the Taylor expansion, and $0<\theta<1$ is a constant dependent on ε. The notation $\boldsymbol{\ell}_N(\boldsymbol{\eta}_N,t,\theta\varepsilon)$ means the value of $\boldsymbol{\ell}_N(\boldsymbol{\eta}_N,t,\varepsilon)$ at any $t\in[t_0,T]$ with the value of its last argument set at $\theta\varepsilon$. Let $X\subset R^3$ be the admissible set of the state $\boldsymbol{x}$ for the system (1–3). Because $\boldsymbol{f}(\boldsymbol{x},u)$ is many times continuously differentiable for all $\boldsymbol{x}\in X$, $\boldsymbol{\ell}_N$ is also smooth and bounded with respect to its arguments, including $\boldsymbol{\eta}_N$. With the expansion (33), Eq. (32) is reduced to

$$\varepsilon^N\dot{\boldsymbol{\eta}}_N = \varepsilon^N(F\boldsymbol{\eta}_N+\boldsymbol{\xi}_N) + \varepsilon^{N+1}\boldsymbol{\ell}_N(\boldsymbol{\eta}_N,t,\theta\varepsilon) \tag{34}$$

Dividing both sides of the preceding equation by ε^N, we have a differential equation for $\boldsymbol{\eta}_N$

$$\dot{\boldsymbol{\eta}}_N(t,\varepsilon) = F\boldsymbol{\eta}_N + [\boldsymbol{\xi}_N + \varepsilon\boldsymbol{\ell}_N(\boldsymbol{\eta}_N,t,\theta\varepsilon)], \qquad \boldsymbol{\eta}_N(t_0,\varepsilon)=0 \tag{35}$$

where the initial condition for η_N in Eq. (35) is from Eq. (31). The solution of the preceding equation, if it exists, can be expressed as

$$\boldsymbol{\eta}_N(t,\varepsilon) = \int_{t_0}^{t}\Phi(t,\tau)\boldsymbol{\xi}_N(\tau)\,\mathrm{d}\tau + \varepsilon\int_{t_0}^{t}\Phi(t,\tau)\boldsymbol{\ell}_N(\boldsymbol{\eta}_N,\tau,\theta\varepsilon)\,\mathrm{d}\tau \tag{36}$$

where the state transition matrix Φ is the same as defined in Sec. IV.A. Because all of the functions involved in the first term of Eq. (36) are smooth and bounded on the finite interval $[t_0,T]$, the first term in Eq. (36) is well defined and bounded for any $t\in[t_0,T]$. Denote the right-hand side of Eq. (36) as a mapping on $\boldsymbol{\eta}_N$ by $\mathcal{M}\boldsymbol{\eta}_N$ so that Eq. (36) can be written in a compact form of $\boldsymbol{\eta}_N=\mathcal{M}\boldsymbol{\eta}_N$. For any two $\boldsymbol{\eta}_N^{(1)}$ and $\eta^{(2)}N$, we have

$$\left\|\mathcal{M}\boldsymbol{\eta}_N^{(1)}(t) - \mathcal{M}\boldsymbol{\eta}_N^{(2)}(t)\right\| = |\varepsilon|\left\|\int_{t_0}^{t}\Phi(t,\tau)\left\{\boldsymbol{\ell}_N\left[\boldsymbol{\eta}_N^{(1)},\tau,\theta\varepsilon\right]\right.\right.$$

$$\left.\left.-\boldsymbol{\ell}_N\left[\boldsymbol{\eta}_N^{(2)},\tau,\theta\varepsilon\right]\right\}\mathrm{d}\tau\right\| \tag{37}$$

where the $\mathcal{L}_\infty$ norm is used. Clearly the distance between the two images $\mathcal{M}\boldsymbol{\eta}_N^{(1)}$ and $\mathcal{M}\boldsymbol{\eta}_N^{(2)}$ can be made arbitrarily small for sufficiently small $|\varepsilon|$. Because $\partial\boldsymbol{\ell}_N/\partial\boldsymbol{\eta}_N$ exists and is continuous, $\boldsymbol{\ell}_N$ is locally Lipschitz in $\boldsymbol{\eta}_N$. Following an argument similar to those used to establish the existence and uniqueness of solutions of differential equations,[14] one can show that for sufficiently small ε, $\mathcal{M}$ is a contraction mapping. Therefore a unique and bounded solution $\boldsymbol{\eta}_N(t,\varepsilon)$ to the fixed-point equation (36) exists on $[t_0,T]$ (Ref. 15). Hence we have $\varepsilon^N\boldsymbol{\eta}_N(t,\varepsilon)\to 0$ as $\varepsilon\to 0$, $\forall t\in[t_0,T]$. By Eq. (30), it follows that

$$\sum_{k=0}^{N-1}\varepsilon^k\boldsymbol{x}_k(t) \to \boldsymbol{x}(t,\varepsilon)$$

as $\varepsilon\to 0$.

In conclusion, the power series in Eq. (15) is indeed asymptotically convergent for all $t\in[t_0,T]$.

V. Analysis of Quasi-Equilibrium Glide Condition

To facilitate the discussion in this section, we first state the notion of the order of a function with respect to a small quantity. Suppose that $q(\varepsilon)$ is continuous function of ε and $q(0)=0$. This function is said to have the order of n with respect to ε for some integer $n\geq 0$ if there exists a constant $c>0$ and $0<\Delta<1$ such that

$$c|\varepsilon|^{n+1} \leq |q(\varepsilon)| \leq c|\varepsilon|^n, \qquad \forall|\varepsilon|\leq\Delta \tag{38}$$

The notation $q=\mathcal{O}(\varepsilon^n)$ signifies the preceding condition. If q is also a continuous function of other variables (such as time) over a compact region, then q in the definition (38) is replaced by the maximum of q with respect to these variables in that region for each fixed ε. The 2-norm of q is used in Eq. (38) if q is a vector.

Under the assumption and qualification given in Sec. III, the asymptotic expansion (15) has been shown to represent the solution to a quasi-equilibrium glide trajectory when $\varepsilon=\varepsilon_0$. Let $(r\ \ V\ \ \gamma)$ be the state and $\sigma(t)$ the actual bank angle profile along this trajectory. We can express the zeroth-order solution in Eq. (15) as

$$r_c(t) = r - \varepsilon_0 r_1 - \varepsilon_0^2 r_2 - \cdots \tag{39}$$

$$V_c(t) = V - \varepsilon_0 V_1 - \varepsilon_0^2 V_2 - \cdots \tag{40}$$

$$\cos\sigma_c = \cos\sigma - \varepsilon_0\delta u \tag{41}$$

Upon substituting the preceding expressions for r_c, V_c, and $\cos\sigma_c$ into the exact equilibrium glide condition in Eq. (8), which is satisfied by the zeroth-order solution, we arrive at

$$L_s\bar{\rho}(r-\varepsilon_0 r_1\cdots)(V-\varepsilon_0 V_1\cdots)^2(\cos\sigma-\varepsilon_0\delta u) + \Big[(V-\varepsilon_0 V_1\cdots)^2$$

$$-1/(r-\varepsilon_0 r_1\cdots)\Big][\cos\gamma_c/(r-\varepsilon_0 r_1\cdots)] = 0 \tag{42}$$

Then expanding the left-hand side of the Eq. (42) in a zeroth-order Taylor series at $\varepsilon_0=0$ and rearranging the equation yield the relationship

$$L_s\bar{\rho}(r)V^2\cos\sigma + (V^2-1/r)(\cos\gamma_c/r) = \mathcal{O}(\varepsilon_0) \tag{43}$$

or more succinctly,

$$L\cos\sigma + (V^2-1/r)(\cos\gamma_c/r) = \mathcal{O}(\varepsilon_0) \tag{44}$$

Note that no simplifications involving the atmospheric model and the aerodynamic model have been required in arriving at Eq. (44). If we expand $\cos\gamma_c = 1-0.5\cos(\nu\gamma_c)\gamma_c^2$ by Taylor series, where $0<\nu<1$ is a constant dependent on γ_c, Eq. (44) can be further reduced to

$$L\cos\sigma + (V^2-1/r)(1/r)$$

$$= \mathcal{O}(\varepsilon_0) + 0.5\gamma_c^2(V^2-1/r)[\cos(\nu\gamma_c)/r] \tag{45}$$

The left-hand side of the preceding equation is exactly the quasi-equilibrium glide condition in Eq. (9). For the case where $\varepsilon_0\neq 0$, γ_c and ε_0 are generally on the same order of magnitude. Hence the right-hand side of Eq. (45) is dominated by $\mathcal{O}(\varepsilon_0)$. The right-hand side of Eq. (45) clearly quantifies the meaning of the prefix "quasi" in the sense that the condition Eq. (9) holds within an accuracy defined by the right-hand side of Eq. (45). Our development, however, accomplishes more than providing a quantifiable accuracy estimate to the QEGC. It also reveals the complete solution structure of lifting entry trajectories in near-equilibrium flight and offers a systematic approach to construct the solution. This fundamental understanding and the construction technique can lead to further compensation to the QEGC. For instance, if a first-order Taylor-series expansion in ε_0 is taken on Eq. (42), we will have, instead of the QEGC in Eq. (9), the following modified QEGC:

$$L\cos\sigma + (V^2-1/r)(1/r) + \varepsilon_0\zeta_1(t) = 0 \tag{46}$$

where $\zeta_1(t)$ is the derivative of the left-hand side of Eq. (42) with respect to ε_0, evaluated at $\varepsilon_0=0$. Assume an exponential atmospheric density model of $\bar{\rho}(r)=\exp[-\beta R_E(r-1)]$, where β is the

reciprocal of a constant density scale height. We can explicitly have

$$\zeta_1(t) = L[(\beta R_E r_1 - 2V_1/V)\cos\sigma - \delta u] + (1/r)\left(V^2 r_1 \Big/ r^2 - 2r_1 \Big/ r^2 - 2VV_1\right) \quad (47)$$

where the functions $r_1(t)$ and $V_1(t)$ are the solution of Eqs. (21) and (22). This modified algebraic relationship in Eq. (46) can be considered a first-order QEGC [whereas Eq. (9) is a zeroth-order QEGC]. The error associated with Eq. (46) is proportional to ε_0^2 when γ_c is on the same order of ε_0. The increased accuracy of Eq. (46) can be very beneficial when higher precision is important in a particular application. Note that there is no more inherent difficulty in applying Eq. (46) than applying Eq. (9) because all of the additional variables r_1, V_1, and δu can be readily generated numerically based on the initial condition of the trajectory and the past history of trajectory control $\sigma(t)$.

Now let us look at some numerical examples of the error estimates when the QEGC in Eq. (9) is used to determine a trajectory parameter. For entry vehicles with medium L/D ratios, γ_c is typically on the order of 10^{-2} (1 deg or less) in magnitude, and ε_0 is on the same order of magnitude. The QEGC contains three variables: r, V, and σ, assuming that the α profile has been specified. The applications of the QEGC inevitably involve finding the value of a variable, given the values of the other two. But one should keep in mind that Eq. (9) is only an approximation. The true expression is Eq. (45), and the dominant residual $\mathcal{O}(\varepsilon_0)$ will cause errors in the computed values.

Consider a typical entry trajectory for the space shuttle at 40 deg of angle of attack. We will use

$$\mathcal{O}(\varepsilon_0) = 5 \times 10^{-2}\ (\mathrm{g})$$

as a representative value for quick demonstrations. The second term on the right-hand side of Eq. (45) is regarded as a higher-order term and ignored. At one point on this trajectory, the relative velocity of the shuttle is 4172 m/s (denoted by V^*). The bank angle at this point is $\sigma^* = -51.1$ deg. Let the left-hand side of Eq. (45), which is the same as the left-hand side of the QEGC, be represented by $\omega(r, V, \sigma)$. Suppose that V^* and σ^* are given as just shown, and the corresponding r is to be estimated from the QEGC in Eq. (9). The obtained value of r^* corresponds to an altitude of 55 km, and that gives an aerodynamic lift acceleration $L^* = 1.126\,g$. But Eq. (45) suggests that the true value of r should be $r = r^* + \Delta r$, and we should have $\omega(r^* + \Delta r, V^*, \sigma^*) = \mathcal{O}(\varepsilon_0)$. The quantity Δr is then the inaccuracy on r when r is estimated from the QEGC. Because $\omega(r^*, V^*, \sigma^*) = 0$, the nondimensional Δr can be found by a first-order Taylor expansion

$$\Delta r \approx \frac{\mathcal{O}(\varepsilon_0)}{\partial\omega(r^*, V^*, \sigma^*)/\partial r} \quad (48)$$

The dimensionless error estimates for ΔV and $\Delta\sigma$ are obtained in similar ways. For computational purposes we use the following exponential atmospheric density model:

$$\rho = 1.72676\exp[-0.150682 \times 10^{-3} R_E(r-1)]\ \mathrm{kg/m^3} \quad (49)$$

This model has about 5% maximum error in the altitude range of 20–120 km when compared to the 1976 U.S. Standard Atmosphere.

1) When the QEGC is used to compute the altitude, the error incurred is

$$\Delta r \approx \frac{\mathcal{O}(\varepsilon_0)}{-0.150682 \times 10^{-3} R_E L^* \cos\sigma^* + (2/r^* - V^{*2})/r^{*2}} = -0.7376 \times 10^{-4} \sim -470.4\ \mathrm{m} \quad (50)$$

2) When the QEGC is used to estimate what the bank angle should be at the point of the trajectory with the given r^* and V^*, the error caused by $\mathcal{O}(\varepsilon_0)$ as seen in Eq. (45) will be

$$\Delta\sigma \approx -\frac{\mathcal{O}(\varepsilon_0)}{L^* \sin\sigma^*} = 0.057\ \mathrm{rad} \sim 3.26\ \mathrm{deg} \quad (51)$$

The process of estimating σ from the QEGC can use some further clarification. Suppose that the values of r and V at a point of the trajectory are given. The bank angle (as the trajectory control) required to achieve these r and V at this point can be estimated by the QEGC, and the preceding computation suggests the accuracy of such an estimate. On a related front, a method of shaping the entry trajectory is to determine the bank angle command from the QEGC based on the values of r and V. In such an application, the discussion of error in QEGC is irrelevant because the QEGC essentially becomes a feedback law for σ, and σ is chosen to satisfy it.

3) When the velocity is computed from the QEGC, the error estimate is

$$\Delta V \approx \frac{\mathcal{O}(\varepsilon_0)}{2(L^* \cos\sigma^*/V^* + V^*/r^*)} = 0.01342 \sim 106.1\ \mathrm{m/s} \quad (52)$$

When the bank angle and velocity at a point of a nearly equilibrium glide trajectory are known, the preceding examples suggest that the corresponding altitude can be determined from the QEGC reasonably accurately. The percentage error in altitude in the preceding case is only about 0.85%. For the bank angle, the difference of a few degrees in σ can be easily compensated by the feedback guidance law that determines the bank angle command. Hence when the altitude and velocity at a point of the trajectory are given, the QEGC can be safely used to calculate the bank angle needed to maintain the trajectory in nearly equilibrium glide. In the design of reference drag profile for the shuttle, the use of QEGC amounts to computing the altitude with given velocity and bank angle.[7] In Ref. 8 the QEGC is used to back out the desired bank angle at given altitude and velocity and to determine the altitude at a given velocity and a specified bank angle. However, the use of the QEGC in Eq. (9) to calculate the value of the velocity at given altitude and bank angle can carry larger percentage errors as the example shows. The error of 106.1 m/s in Eq. (52) already represents an inaccuracy of 2.54%. Thus care should be exercised when the QEGC is employed to estimate the velocity at the given altitude and bank angle.

The foregoing error analysis utilizes $\mathcal{O}(\varepsilon_0)$, a quantity of order one with respect to ε_0. Even though the exact value of ε_0 is dependent on γ_c as in Eq. (10), which is not explicitly given, the range of the possible values for γ_c can be easily determined, given the interval of interest $[t_0, T]$ and the specified initial conditions $r^{(0)}$ and $V^{(0)}$ (see the example in the next section). Therefore the maximum of ε_0 can be obtained once $\gamma^{(0)}$ is specified. As a result, the order of magnitude of $\mathcal{O}(\varepsilon_0)$ along the trajectory can be estimated and used to establish the error bounds of the variables from the QEGC.

It is recognized that other traditional uncertainties, such as those in aerodynamic modeling, atmospheric properties, and navigation data, will all result in inaccuracy in the use of the QEGC. This paper only addresses the approximation effects arising from flight mechanics.

VI. Recapitulation and Numerical Illustrations

When a lifting entry trajectory is well designed in that it has no large or rapid oscillations in altitude and carries no excessive heat and load penalty, the trajectory will have relatively slowly varying (and small) flight-path angle in that part of flight. The QEGC [Eq. (9)] will be met in an extended period of time within the accuracy estimated by the right-hand side of Eq. (45). An especially useful function of QEGC is in shaping entry trajectories. The part of the trajectory designed on the basis of satisfying the QEGC [Eq. (9)] will necessarily have slowly varying flight-path angle and little or no altitude phugoid oscillations, provided that the initial flight-path angle is within a proper range. Such applications are the centerpiece of the trajectory planning algorithm in Ref. 8. It is hence not a surprise that the trajectory so designed typically has a well-behaved, nonoscillatory altitude history in the portion of the trajectory where the QEGC is in force.[8]

The assumption and the qualifying condition in Sec. III on quasi-equilibrium glide suggest that the QEGC should not be regarded as a naturally occurring phenomenon under all circumstances. One

should not expect that the profiles of r, V, σ, and C_L along an arbitrary lifting entry trajectory will necessarily satisfy the QEGC in Eq. (9) with acceptable accuracy. The QEGC should be taken as a designed outcome, rather than an approximate motion integral that is always valid.

We conclude this section with numerical illustrations of the development in Secs. IV and V. The space shuttle vehicle data and aerodynamic model are used in the following numerical results. The coefficients C_L and C_D are functions of Mach number and angle of attack. The entry flight begins at the entry interface at the altitude of 122 km (400,000 ft). The initial conditions for our numerical experiments are chosen to be those along a typical entry trajectory at about $t_0 = 400$ s after the entry interface:

$$r^{(0)} \sim 76.151 \text{ km}, \qquad V^{(0)} \sim 7{,}463 \text{ m/s}, \qquad \gamma^{(0)} \sim -0.069 \text{ deg} \tag{53}$$

The α profile is given as a typical Mach-dependent profile flown by the shuttle. It is easy to verify by numerical integration that starting at the preceding altitude and velocity any choice of γ_c within

$$-0.55 \text{ deg} \le \gamma_c \le -0.15 \text{ deg}$$

will satisfy the assumption in Sec. III for a period of $T - t_0 = 600$ s. A value of $\gamma_c = -0.25$ deg is selected for the following computation. For the preceding $\gamma^{(0)}$ and this γ_c, $\varepsilon_0 = 0.32 \times 10^{-2}$ rad. For this γ_c, the corresponding equilibrium glide bank angle profile $\sigma_c(t)$ is shown in Fig. 1. The actual bank angle to be flown is assumed to be a constant at $\sigma = 45$ deg in $[t_0, T]$. From Fig. 1 it is evident that $\sigma_c(t)$ and σ are quite different. Yet the condition in Eq. (12) is met with a $k \approx 0.2$. So the actual trajectory can be regarded as in quasi-equilibrium glide, and a truncated expansion based on (15) should represent the trajectory closely. We will examine the first three terms in Eq. (15). The solutions for $\boldsymbol{x}_0(t)$, $\boldsymbol{x}_1(t)$, and $\boldsymbol{x}_2(t)$ are numerically generated according to their respective differential equations given in Sec. IV. The truncated trajectory solutions at zeroth order represented by $\boldsymbol{x}_0(t)$, first order by $\boldsymbol{x}_0(t) + \varepsilon_0 \boldsymbol{x}_1(t)$, and second order by $\boldsymbol{x}_0(t) + \varepsilon_0 \boldsymbol{x}_1(t) + \varepsilon_0^2 \boldsymbol{x}_2(t)$ are constructed. The bank angle $\sigma = 45$ deg is used together with the specified α profile to numerically integrate Eqs. (1–3) with the initial conditions in Eq. (53). The solution so obtained is referred to as the full solution.

Figure 2 shows the comparison of altitude histories in the zeroth-, first-, second-order solutions, and the full solution. The first-order solution is already quite close to the full solution, and the second-order solution is almost indiscernible from the full solution. Note that the zeroth-order solution is not a "steady-state solution" in the sense that the true (full) solution approaches to it as time progresses, as can seen from Fig. 2. This is because the perturbation solutions are for a regular perturbation problem, not a singular perturbation problem, which has an outer (asymptotic) solution. The same comment applies to other variables. The velocity histories are plotted

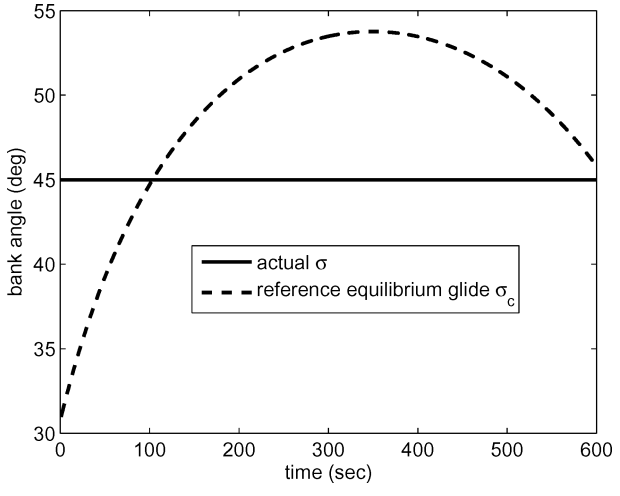

Fig. 1 Bank angle profiles.

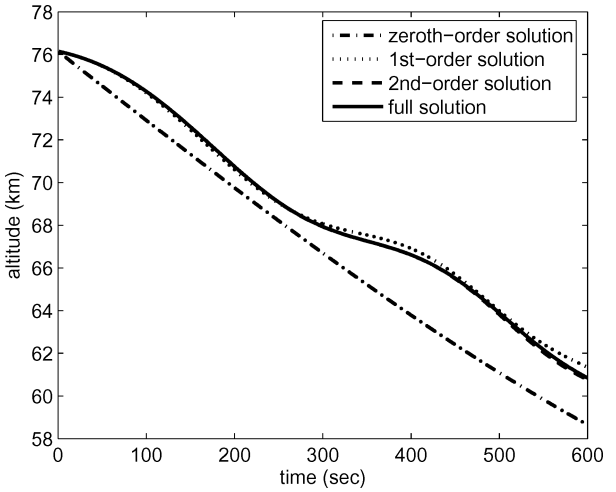

Fig. 2 Comparison of altitude histories.

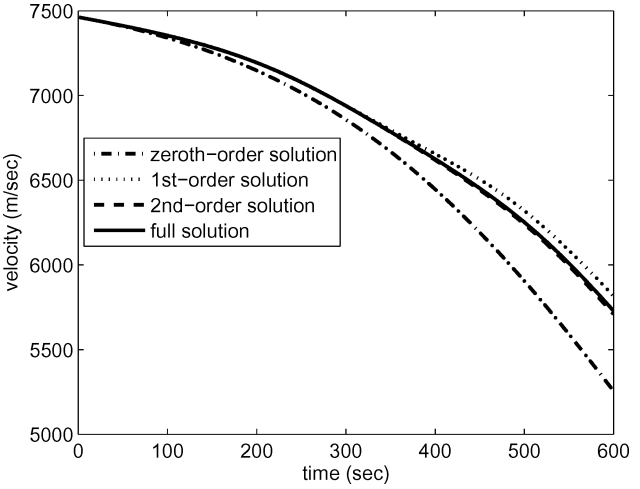

Fig. 3 Comparison of velocity histories.

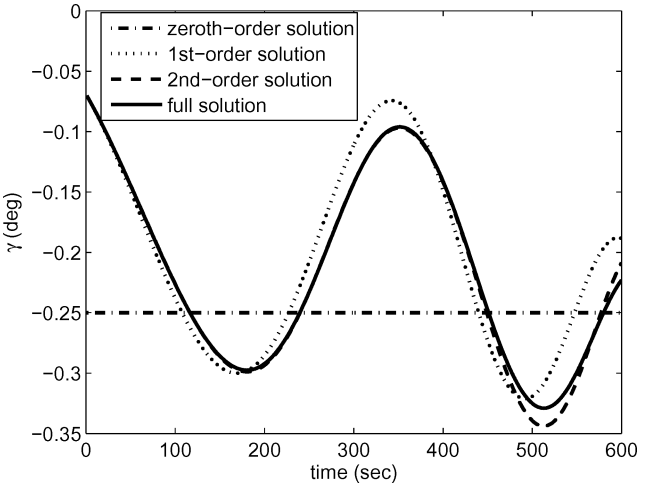

Fig. 4 Comparison of flight-path angle histories.

in Fig. 3. Again the first-order solution is reasonably close, and the second-order solution is practically the same as the full solution. More visible differences can be observed in Fig. 4, where the variations of the flight-path angles are depicted (notice the small scale on the y axis, though). Compared with the zeroth-order solution (at constant $\gamma_0 = \gamma_c$), the first-order solution for the flight-path angle begins to capture the trend of the variation of the full solution, but it exhibits an apparent phase shift. The second-order solution corrects this phase mismatch and makes up for most of the magnitude

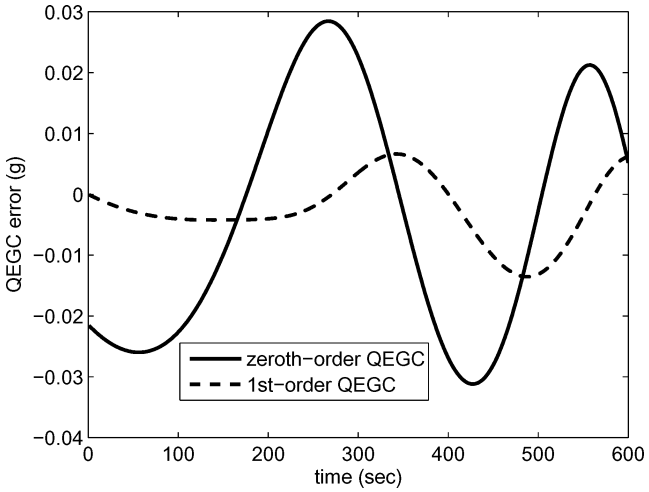

Fig. 5 Error of quasi-equilibrium glide condition along the actual trajectory.

differences. In all of the three state variables, the exact equilibrium glide (zeroth-order) solutions are rather far from the full solutions and thus cannot reasonably approximate the actual trajectory. On the other hand, the second-order solutions compensate most of the inaccuracy in the zeroth-order solutions (this, of course, is dependent on the sizes of ε_0 and δu).

Figure 5 illustrates the residuals incurred by the zeroth-order QEGC in Eq. (9) and the modified (first-order) QEGC in Eq. (46) along the full solution of the trajectory. The error for the zeroth-order QEGC is defined to be

$$\text{zeroth-order QEGC error} = L\cos\sigma + (V^2 - 1/r)(1/r) \tag{54}$$

and the error for the first-order QEGC is

$$\text{first-order QEGC error} = L\cos\sigma + (V^2 - 1/r)(1/r) + \varepsilon_0\zeta_1(t) \tag{55}$$

where $\zeta_1(t)$ is given by Eq. (47). The errors are in g as all of the variables in the preceding equations are nondimensional. It can be seen from Fig. 5 that the maximum magnitude of the error in the zeroth-order QEGC is about $3.2 \times 10^{-2}\ g$ [recall that a similar value, $5 \times 10^{-2}\ g$, is used for the magnitude of $\mathcal{O}(\varepsilon_0)$ in Sec. V to demonstrate numerically the accuracy of the QEGC]. The first-order QEGC, on the other hand, carries a much smaller error whose maximum magnitude is no greater than $1.5 \times 10^{-2}\ g$. Therefore in this case, any estimates of the trajectory variables based on the first-order QEGC in Eq. (46) will have significantly smaller inaccuracy than those from the zeroth-order QEGC in Eq. (9).

VII. Conclusions

The quasi-equilibrium glide condition (QEGC) is an approximate equation in lifting entry flight and has been a very useful tool in entry flight mechanics and guidance designs. In this paper we provide a formal treatment of quasi-equilibrium gliding flight. Using a regular perturbation approach, we have established that the longitudinal trajectory in quasi-equilibrium glide can be represented by the sum of an exact equilibrium glide solution and other higher-order solutions. The problem and solution are characterized by a small parameter that defines the closeness of the trajectory to an exact equilibrium glide trajectory. Our analysis leads to quantifiable accuracy estimate to the QEGC, which in turn helps determine the estimation errors when the trajectory variables are obtained from the QEGC. In case where higher precision is needed, a modification to the traditional QEGC can markedly increase the accuracy on the basis of the asymptotic solution we have obtained.

Appendix: Examples of Expansion Expressions

Denote the right hands of Eqs. (1), (2), and (3) by f_r, f_V, and f_γ, respectively. The matrix $F(t) \in R^{3\times 3}$, first appearing in Eq. (17), is defined by

$$F(t) = \left.\begin{pmatrix} \partial f_r/\partial r & \partial f_r/\partial V & \partial f_r/\partial\gamma \\ \partial f_V/\partial r & \partial f_V/\partial V & \partial f_V/\partial\gamma \\ \partial f_\gamma/\partial r & \partial f_\gamma/\partial V & \partial f_\gamma/\partial\gamma \end{pmatrix}\right|_{x=x_0(t)} \tag{A1}$$

Approximate the normalized atmospheric density by an exponential model

$$\bar\rho(r) = \exp[-\beta R_E(r-1)] \tag{A2}$$

where β is the reciprocal of a constant density scale height. For the Earth, $\beta R_E \approx 920$ (see Ref. 3). If we ignore the variations of C_L and C_D with Mach number (but these simplifications are not necessary), the matrix $F(t)$ takes the following form:

$$F(t) = \begin{pmatrix} 0 & \sin\gamma_c & V_0\cos\gamma_c \\ \beta R_E D_s\bar\rho(r_0)V_0^2 + 2\sin\gamma_c/r_0^3 & -2D_s\bar\rho(r_0)V_0 & -\cos\gamma_c/r_0^2 \\ F_{31} & F_{32} & F_{33} \end{pmatrix} \tag{A3}$$

where

$$F_{31} = -\beta R_E L_s\bar\rho(r_0)V_0\cos\sigma_c + (2/r_0V_0 - V_0)\left(\cos\gamma_c/r_0^2\right) \tag{A4}$$

$$F_{32} = L_s\bar\rho(r_0)\cos\sigma_c + \left(1 + 1/r_0V_0^2\right)(\cos\gamma_c/r_0) \tag{A5}$$

$$F_{33} = (1/r_0V_0 - V_0)(\sin\gamma_c/r_0) \tag{A6}$$

Again, $r_0(t) = r_c(t)$ and $V_0(t) = V_c(t)$ are obtained from the zeroth-order solution defined in Eqs. (6) and (7) and $\cos\sigma_c = u_c$ from Eq. (8).

From Eqs. (17) and (19), the expression for $\boldsymbol{\xi}_2 = [\xi_2^{(1)}\ \ \xi_2^{(2)}\ \ \xi_2^{(3)}]^T$ is

$$\boldsymbol{\xi}_2 = \frac{1}{2!}\left\{\frac{\mathrm{d}F[\boldsymbol{x}(t,\varepsilon),u_c]}{\mathrm{d}\varepsilon}\frac{\partial\boldsymbol{x}}{\partial\varepsilon} + \frac{\mathrm{d}\boldsymbol{\xi}_1[\boldsymbol{x}(t,\varepsilon),\delta u]}{\mathrm{d}\varepsilon}\right\}_{\varepsilon=0}$$

$$= \frac{1}{2}\left.\frac{\mathrm{d}F[\boldsymbol{x}(t,\varepsilon),u_c]}{\mathrm{d}\varepsilon}\right|_{\varepsilon=0}\boldsymbol{x}_1 + \frac{1}{2}\left.\frac{\partial\boldsymbol{\xi}_1[\boldsymbol{x}(t,\varepsilon),\delta u]}{\partial\boldsymbol{x}}\frac{\partial x}{\partial\varepsilon}\right|_{\varepsilon=0} \tag{A7}$$

After carrying out the differentiations and algebraic operations, we have in componentwise form

$$\xi_2^{(1)} = -\frac{1}{2}(V_0\sin\gamma_c)\gamma_1^2 + (\cos\gamma_c)V_1\gamma_1 \tag{A8}$$

$$\xi_2^{(2)} = -\frac{1}{2}\left[(\beta R_E)^2D_0 + \frac{6\sin\gamma_c}{r_0^4}\right]r_1^2 - \frac{D_0}{V_0^2}V_1^2 + \frac{\sin\gamma_c}{2r_0^2}\gamma_1^2 + 2\frac{\beta R_E D_0}{V_0}r_1V_1 + 2\frac{\cos\gamma_c}{r_0^3}r_1\gamma_1 \tag{A9}$$

$$\xi_2^{(3)} = \frac{1}{2}\left[\frac{(\beta R_E)^2L_0\cos\sigma_c}{V_0} + \left(2V_0 - \frac{6}{r_0V_0}\right)\frac{\cos\gamma_c}{r_0^3}\right]r_1^2 - \frac{\cos\gamma_c}{r_0^2V_0^3}V_1^2 + \frac{1}{2}\left[\left(\frac{1}{r_0V_0} - V_0\right)\frac{\cos\gamma_c}{r_0}\right]\gamma_1^2 - \left[\frac{\beta R_E L_0\cos\sigma_c}{V_0^2} + \left(1 + \frac{2}{r_0V_0^2}\right)\frac{\cos\gamma_c}{r_0^2}\right]r_1V_1 - \left[\left(\frac{2}{r_0V_0} - V_0\right)\frac{\sin\gamma_c}{r_0^2}\right]r_1\gamma_1 - \left[\left(1 + \frac{1}{r_0V_0^2}\right)\frac{\sin\gamma_c}{r_0}\right]V_1\gamma_1 + \frac{1}{2}\left(-\beta R_E\frac{r_1}{V_0} + \frac{V_1}{V_0^2}\right)L_0\delta u \tag{A10}$$

where in the peceding $D_0 = D_s\bar\rho(r_0)V_0^2$, $L_0 = L_s\bar\rho(r_0)V_0^2$, and δu is defined in Eq. (11).

References

[1]Sänger, E., *Raketen-Flugtechnik*, R. Oldenbourg, Berlin, 1933.

[2]Sänger, E., and Bredt, J., "A Rocket Drive for Long Range Bombers," Deutsche Luftfahrtforschung UM 3538, 1944; Technical Information Branch, Navy Dept., Washington, DC, translation CGD-32.

[3]Chapman, D. R., "An Approximate Analytical Method for Studying Entry into Planetary Atmospheres," NACA TN-4276, May 1958.

[4]Eggers, A. J., Jr., Allen, H. J., and Niece, S. E., "A Comparative Analysis of the Performance of Long-Range Hypervelocity Vehicles," NACA TN 4046, 1957.

[5]Shkadov, L. M., Bukhanova, R. S., Illarionov, V. F., and Plokhikh, V. P., "Mechanics of Optimum Three-Dimensional Motion of Aircraft in the Atmosphere," NASA TT F-777, March 1975.

[6]Vinh, N. X., *Optimal Trajectories in Atmospheric Flight*, Elsevier Scientific, New York, 1981, pp. 340, 349.

[7]Harpold, J. C., and Graves, C. A., "Shuttle Entry Guidance," *The Journal of the Astronautical Sciences*, Vol. XXXVII, No. 3, 1979, pp. 239–268.

[8]Shen, Z., and Lu, P., "On-Board Generation of Three-Dimensional Constrained Entry Trajectories," *Journal of Guidance, Control, and Dynamics*, Vol. 26, No. 1, 2003, pp. 111–121.

[9]Lin, C. C., and Segel, L. A., *Mathematics Applied to Deterministic Problems in the Natural Sciences*, Collier Macmillan, New York, 1974, pp. 209–222.

[10]Shi, Y. Y., and Pottsepp, L., "Asymptotic Expansions of a Hypervelocity Atmospheric Entry Problem," *AIAA Journal*, Vol. 7, No. 2, 1969, pp. 353–355.

[11]Busemann, A., Vinh, N. X., and Culp, R. D., "Solution of the Exact Equations for Three-Dimensional Atmospheric Entry Using Directly Matched Asymptotic Expansion," NASA Report CR-2643, March 1976.

[12]Naidu, D. S., "Three-Dimensional Atmospheric Entry Problem Using Method of Matched Asymptotic Expansions," *IEEE Transactions on Aerospace and Electronic Systems*, Vol. 25, No. 5, 1989, pp. 660–667.

[13]Naidu, D. S., and Calise, A. J., "Singular Perturbations and Time Scales in Guidance and Control of Aerospace Systems: A Survey," *Journal of Guidance, Control and Dynamics*, Vol. 24, No. 6, 2001, pp. 1057–1078.

[14]Naylor, A. W., and Sell, G. R., *Linear Operator Theory in Engineering and Science*, Springer-Verlag, New York, 1982, pp. 51, 126, 127.

[15]O'Malley, R. E., Jr., *Singular Perturbation Methods for Ordinary Differential Equations*, Springer-Verlag, New York, 1991, pp. 17–20.